Electronic Properties of N-Heterocyclic Carbene (NHC) Ligands: Synthetic, Structural, and Spectroscopic Studies of (NHC)Platinum(II) Complexes

Serena Fantasia,[†,⊥] Jeffrey L. Petersen,[‡] Heiko Jacobsen,[§] Luigi Cavallo,[∥] and Steven P. Nolan*[,†]

Institute of Chemical Research of Catalonia (ICIQ), Av. Països Catalans 16, 43007 Tarragona, Spain, C. Eugene Bennett Department of Chemistry, West Virginia University, Morgantown, West Virginia 26506-6045, KemKom, Libellenweg 2, 25917 Leck, Germany, and Department of Chemistry, Università di Salerno, Via Ponte don Melillo, Fisciano (SA), I-84084, Italy

Received August 28, 2007

N-Heterocyclic carbene complexes of platinum(II) have been synthesized, notably monocarbene complexes *cis*-[(IPr)Pt(dmso)(Cl)$_2$], **6**, *cis*-[(IMes)Pt(dmso)(Cl)$_2$], **7**, *cis*-[(SIPr)Pt(dmso)(Cl)$_2$], **8**, *cis*-[(SIMes)Pt(dmso)(Cl)$_2$], **9**, and *cis*-[(TTP)Pt(dmso)(Cl)$_2$], **10**. All complexes have been fully characterized by multinuclear NMR spectroscopy. Complex **7**, **9**, and **10** have been characterized by X-ray crystallography. The data obtained have allowed for the differentiation between electronic contributions (σ and π) present in the Pt−NHC bond. Supported by computational analyses, the percentage of π back-donation from the metal to the NHC is found to be on the order of 10%. More interestingly, we find that saturated NHC (SIPr and SIMes) are more efficient π back-acceptors than their unsaturated NHC congeners (IPr and IMes). The synergistic effect between π back-donation and σ donation present in the saturated NHC systems results in increased electron density at the platinum center compared to the bonding situation in the unsaturated NHC examples.

Introduction

In the recent past, the use of N-heterocyclic carbenes (NHCs) as ligands in coordination chemistry has attracted considerable attention.[1] Many important reactions, such as olefin metathesis,[2] Pd-catalyzed cross-coupling reactions,[3] and hydrogenation reactions,[4] have shown marked improvements with the use of novel NHC−metal complexes. The main characteristic of this class of ligands is its strong σ donor property, even stronger than alkyl phosphines; ligand steric properties are also quite different than those of phosphines. These properties lead in many cases to a greater stability of the catalysts or precatalysts.[5] In view of their increasing popularity, much effort has been focused on understanding their stereoelectronic properties[6] in order to guide catalyst design studies. Despite the fact that it is now well recognized that NHC ligands are stronger σ donor than phosphines, our knowledge of this class of ligands is still limited and a classification of the properties of the many different NHCs is lacking. Rationalizing their different properties is particularly important if we think that in many systems replacing one NHC by another significantly varies the activity of the catalyst.[7] A recent study by Plenio[6c] also shows that redox potential in NHC−Ru complexes of Grubbs−Hoveyda type varies substantially from saturated to unsaturated NHCs. Our group has been

* Corresponding author. E-mail: snolan@iciq.es.
† Institute of Chemical Research of Catalonia.
‡ West Virginia University.
§ KemKom.
∥ Università di Salerno.
⊥ Visiting student from Università degli Studi di Milano, Via Venezian 21, 20133 Milano, Italy.

(1) (a) Nolan, S. P., Ed. *N-Heterocyclic Carbenes in Synthesis*; Wiley-VCH: Weinheim, Germany, 2006. (b) Glorius, F. *N-Heterocyclic Carbenes in Transition Metal Catalysis*; Springer: Berlin, 2007.

(2) (a) Weskamp, T.; Schattenmann, W. C.; Spiegler, M.; Herrmann, W. A. *Angew. Chem., Int. Ed.* **1998**, *37*, 2490−2493. (b) Huang, J.; Stevens, E. D.; Nolan, S. P.; Petersen, J. L. *J. Am. Chem. Soc.* **1999**, *121*, 2674−2678. (c) Scholl, M.; Ding, S.; Lee, C. W.; Grubbs, R. H. *Org. Lett.* **1999**, *1*, 953−956. (d) Huang, J.; Stevens, E. D.; Nolan, S. P. *Organometallics* **2000**, *19*, 1194−1197. (e) Choi, T.-L.; Grubbs, R. H. *Angew. Chem., Int. Ed.* **2003**, *42*, 1743−1746.

(3) (a) Grasa, G. A.; Viciu, M. S.; Huang, J.; Nolan, S. P. *J. Org. Chem.* **2001**, *66*, 7729−7737. (b) Grasa, G. A.; Viciu, M. S.; Huang, J.; Zhang, C.; Trudell, M. L.; Nolan, S. P. *Organometallics* **2002**, *21*, 2866−2873. (c) Navarro, O.; Kelly, R. A., III; Nolan, S. P. *J. Am. Chem. Soc.* **2003**, *125*, 16194−16195. (d) Marion, N.; Navarro, O.; Mei, J.; Stevens, E. D.; Scott, N. M.; Nolan, S. P. *J. Am. Chem. Soc.* **2006**, *128*, 4101−4111. (e) Navarro, O.; Marion, N.; Mei, J. Nolan, S. P. *Chem.−Eur. J.* **2006**, *12*, 5142−5148. (f) Lock, J. A.; Albrecht, M.; Peris, E.; Mata, J.; Faller, J. W.; Crabtree, R. H. *Organometallics* **2002**, *21*, 700−706. (g) Gründemann, S.; Albrecht, M.; Loch, J. A.; Faller, J. W.; Crabtree, R. H. *Organometallics* **2001**, *20*, 5485−5488. (h) Peris, E.; Loch, J. A.; Mata, J.; Crabtree, R. H. *Chem. Commun.* **2001**, 201−202. (i) Gstöttmayr, C. W. K.; Böhm, V. P. W.; Herdtweck, E.; Grosche, M.; Herrmann, W. A. *Angew. Chem., Int. Ed.* **2002**, *41*, 1363−1365.

(4) (a) Hillier, A. C.; Lee, H. M.; Stevens, E. D.; Nolan, S. P. *Organometallics* **2001**, *20*, 4246−4252. (b) Vasquez-Serrano, L. D.; Owens, B. T.; Buriak, J. M. *Chem. Commun.* **2002**, 2518−2519. (c) Sprengers, J. W.; Wassenaar, J.; Clément, N. D.; Cavell, K. J.; Elsevier, C. J. *Angew. Chem., Int. Ed.* **2005**, *44*, 2026−2029. (d) Dharmasena, U. L.; Foucault, H. M.; Dos Santos, E. N.; Fogg, D. E.; Nolan, S. P. *Organometallics* **2005**, *24*, 1056−1058. (e) Albrecht, M.; Crabtree, R. H.; Mata, J.; Peris, E. *Chem. Commun.* **2002**, 32−33. (f) Albrecht, M.; Miecznikowski, J. R.; Samuel, A.; Faller, J. W.; Crabtree, R. H. *Organometallics* **2002**, *21*, 3596−3604.

(5) (a) Bourissou, D.; Guerret, O.; Gabbaï, F. P.; Bertrand, G. *Chem. Rev.* **2000**, *100*, 39−91. (b) Herrmann, W. A. *Angew. Chem., Int. Ed.* **2002**, *41*, 1290−1309. (c) Díez-González, S.; Nolan, S. P. *Coord. Chem. Rev.* **2007**, *251*, 874−883.

(6) (a) Hillier, A. C.; Sommer, W. J.; Yong, B. S.; Petersen, J. L.; Cavallo, L.; Nolan, S. P. *Organometallics* **2003**, *22*, 4322−4326. (b) Magill, A. M.; Cavell, K. J.; Yates, B. F. *J. Am. Chem. Soc.* **2004**, *126*, 8717−8724. (c) Süβner, M; Plenio, H. *Chem. Commun.* **2005**, 5417−5419. (d) Dorta, R.; Stevens, E. D.; Scott, N. M.; Costabile, C.; Cavallo, L.; Hoff, C. D.; Nolan, S. P. *J. Am. Chem. Soc.* **2005**, *127*, 2485−2495. (e) Perrin, L.; Clot, E.; Eisenstein, O.; Loch, J.; Crabtree, R. H. *Inorg. Chem.* **2001**, *40*, 5806−5811. (f) Mata, J. A.; Chianese, A. R.; Miecznikowski, J. R.; Poyatos, M. Peris, E. Faller, J. W.; Crabtree, R. H. *Organometallics* **2004**, *23*, 1253−1263.

10.1021/om700857j CCC: $37.00
Publication on Web 10/26/2007

particularly active in trying to define parameters that could explain the different behavior among NHC ligands. Of particular interest has been the differences between the saturated and the unsaturated NHCs. Notably, we have reported on the dissociation energy of NHCs in the [(Cp*)Ru(NHC)Cl] system,[6a] in which a very small difference of 4 kJ mol^{-1} was found between a saturated (SIMes) and an unsaturated congener (IMes) NHC, suggesting that the first are better donors, but only slightly. More recently, [(NHC)Ni$(CO)_3$] complexes have been synthesized and their infrared carbonyl stretching frequencies recorded,[6d] but even in this system, the difference in the IR frequencies among the different NHC complexes is very small and renders difficult an unambiguous understanding of electronic properties. Moreover recent studies have shown that despite the NHCs being strong σ donor ligands, ignoring other types of stereoelectronic metal−ligand interactions is an oversimplification of the bonding picture.[8]

Wanting to shed light on this point, we have synthesized a family of NHC−Pt(II) complexes bearing simple, minimally π-accepting ligands without the presence of a strong π acceptor such as CO. The investigation of the [(NHC)Pt(dmso)$(Cl)_2$] system, (dmso = dimethylsulfoxide), easily accessible with a variety of NHC ligands by simple ligand substitution, allows for detailed spectroscopic and structural X-ray diffraction studies. This system has the added feature of possessing a NMR-active Pt center whose chemical shift and *J* coupling with the carbenic carbon can provide useful bonding information and may enable differentiation of the electronic contribution to the M−C bond. Indeed analogous studies on tertiary phosphine systems have led to a better understanding of the nature of bonding interactions between PR_3 and metals.[9] NMR studies on platinum−phosphine systems have led to the separation of the σ and the π electronic contributions in the M−L (L = ligand) bond.[10] Such fundamental understanding has had a major impact on the design of new phosphine ligands for catalytic uses. The present data allow us to characterize the different contribution displayed by NHCs when they bind this metal. In particular we have been able to qualitatively define the relative magnitude of σ donation and π back-donation for saturated and unsaturated NHCs. Analysis of X-ray diffraction metrical parameters associated with the Pt−Cl bond length in these complexes allows the NHC ligands to be positioned on the *trans* influence scale.[11]

Results and Discussion

The stoichiometric reaction between *cis*-[Pt$(dmso)_2(Cl)_2$] and 1 equiv of N-heterocyclic carbenes (NHC), depicted in Figure 1, leads to complexes of general formula *cis*-[(NHC)(Pt)(dmso)$(Cl)_2$] (eq 1). The reaction of 1 equiv of IPr (1,3-bis(2,6-diisopropyl)phenyl imidazol-2-ylidene), **1**, IMes (1,3-bis(2,4,6-trimethyl)phenyl imidazol-2-ylidene), **2**, SIPr (1,3-bis(2,6-diisopropyl)phenyl-4,5-dihydroimidazol-2-ylidene), **3**, SIMes (1,3-bis(2,4,6-trimethyl)phenyl-4,5-dihydroimidazol-2-ylidene), **4**, and TTP (TTP = 1,3,4-triphenyl-1,2,4-triazol-5-ylidene), **5**, with the precursor *cis*-[Pt$(dmso)_2(Cl)_2$] leads to the substitution of one dmso ligand. The monocarbenic complexes *cis*-[(IPr)Pt$(dmso)(Cl)_2$], **6**, *cis*-[(IMes)Pt$(dmso)(Cl)_2$], **7**, *cis*-[(SIPr)Pt$(dmso)(Cl)_2$], **8**, *cis*-[(SIMes)Pt$(dmso)(Cl)_2$], **9**, and *cis*-[(TTP)Pt$(dmso)(Cl)_2$], **10**, are obtained as microcrystalline white solids in good yields. All complexes, presented in Figure 2, have been fully characterized by ^1H, ^{13}C, and ^{195}Pt NMR spectroscopy. To further confirm the geometrical arrangement and bonding around the metal center, X-ray diffraction studies were carried out on complexes [(IMes)Pt$(dmso)(Cl)_2$], **7**, [(SIMes)Pt$(dmso)(Cl)_2$], **9**, and [(TTP)Pt$(dmso)(Cl)_2$], **10**.[12]

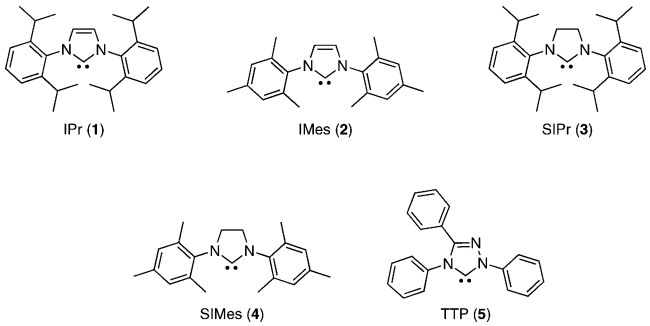

Figure 1. NHCs utilized in the present study.

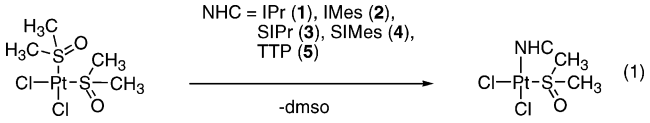

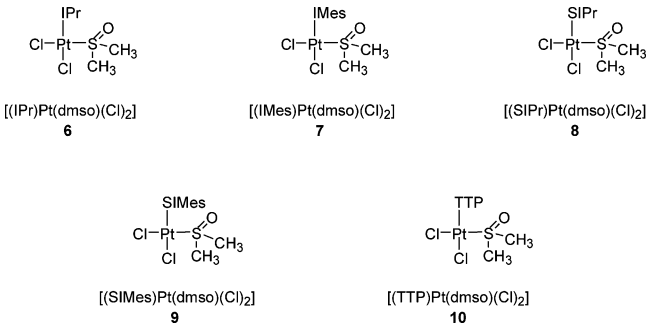

Figure 2. [(NHC)Pt$(dmso)(Cl)_2$] complexes.

X-ray Structures. Suitable crystals for X-ray analysis were grown by slow diffusion of hexane in a saturated chloroform solution of the compounds. Crystallographic data for **7**, **9**, and **10** are reported in Table 1. Relevant bond distances and angles are reported in Table 2, while ball-and-stick representations for **7** [(IMes)Pt$(dmso)(Cl)_2$], **9** [(SIMes)Pt$(dmso)(Cl)_2$], and **10** [(TTP)Pt$(dmso)(Cl)_2$] are presented in Figure 3. The complexes show the expected square-planar geometry around the platinum, even if the steric hindrance of the NHCs causes a widening of the S(1)−Pt−C(1) angle of about 6° in the compounds IMes **7** and SIMes **9**, while in the less sterically demanding TTP **10**

(7) See for example: (a) De Bo, G.; Bretón-Gelloz, G.; Tinant, B.; Markó, I. E. *Organometallics* **2006**, *25*, 1881−1890. (b) Viciu, M. S.; Navarro, O.; Germaneau, R. F.; Nelly, R. A., III; Sommer, W.; Marion, N.; Stevens, E. D.; Cavallo, L.; Nolan, S. P. *Organometallics* **2004**, *23*, 1629−1635. (c) Ackermann, L.; Fürstner, A.; Weskamp, T.; Kohl, F. J.; Herrmann, W. A. *Tetrahedron Lett.* **1999**, *40*, 4787−4790.

(8) (a) Tulloch, A. D. D.; Danopoulos, A. A.; Kleinhenz, S.; Light, M. E.; Hursthouse, M. B.; Eastham, G. *Organometallics* **2001**, *20*, 2027−2031. (b) Hu, X. L.; Tang, Y. J.; Gantzel, P.; Meyer, K. *Organometallics* **2004**, *23*, 612−614. (c) Hu, X. L.; Castro-Rodriguez, I.; Olsen, K.; Meyer, K. *Organometallics* **2004**, *23*, 755−764. (d) Nemcsok, D.; Wichmann, K.; Frenking G. *Organometallics* **2004**, *23*, 3640−3646. (e) Scott, N. M.; Dorta, R.; Stevens, E. D.; Correa, A.; Cavallo, L.; Nolan, S. P. *J. Am. Chem. Soc.* **2005**, *127*, 3516−3526.

(9) Tolman, C. A. *Chem. Rev.* **1977**, *77*, 313−348.

(10) Cobley, C. J.; Pringle, P. G. *Inorg. Chim. Acta* **1997**, *265*, 107−115.

(11) (a) Bugarcic, Z.; Lövqvist, K.; Oskarsson, Å. *Acta Chem. Scand.* **1992**, *46*, 854−860. (b) Kapoor, P.; Kukushkin, V. Y.; Lövqvist, K.; Oskarsson, Å. *J. Organomet. Chem.* **1996**, *517* ,71−79. For a review on *trans* influence in Pt(II) complexes see: (c) Dedieu, A. *Chem. Rev.* **2000**, *100*, 543−600.

(12) Structural analysis of the entire series was not possible, as X-ray quality crystals for **6** and **8** were not obtained, this even after numerous crystallization attempts.

Table 1. Crystallographic Data for Complexes 7, 9, and 10

	[(IMes)Pt(dmso)(Cl)$_2$], **7**	[(SIMes)Pt(dmso)(Cl)$_2$], **9**	[(TTP)Pt(dmso)(Cl)$_2$], **10**
chemical formula	$C_{23}H_{30}Cl_2N_2OPtS$	$C_{23}H_{32}Cl_2N_2OPtS$	$C_{22}H_{20}Cl_2N_3OPtS$
M (g/mol)	648.54	650.56	640.46
T (K)	293(2)	293(2)	100(2)
cryst syst	monoclinic	monoclinic	orthorhombic
space group	$P2_1/c$	$P2_1/c$	*Pbcn*
a (Å)	10.490(1)	10.8158(10)	29.6172(15)
b (Å)	13.580(2)	14.0465(12)	9.6056(5)
c (Å)	18.082(2)	17.2816(15)	16.3161(8)
α (deg)	90	90	90
β (deg)	104.939(2)	107.298(2)	90
γ (deg)	90	90	90
V (Å^3)	2488.6(5)	2506.7(4)	4641.8(4)
Z	4	4	8
d(calcd) (g cm^{-3})	1.731	1.724	1.833
absorp coeff (mm^{-1})	59.54	59.11	6.385
F(000)	1272	1280	2472
cryst size (mm)	0.10 × 0.22 × 0.24	0.26 × 0.30 × 0.36	0.20 × 0.05 × 0.05
θ (deg)	1.90 to 27.57	1.90 to 27.54	2.82 to 39.63
index range *hkl*	−13 to +11, −17 to +17, −23 to +22	−12 to +13, −17 to +18, −20 to +22	−51 to +49, −17 to +12, −29 to +28
no. of data/restraints/params	5616/2/279	5548/0/279	13 711/0/351
goodness-of-fit on F^2	1.046	1.046	1.131
final *R* values	$R_1 = 0.0564$ $wR_2 = 0.1496$	$R_1 = 0.0407$ $wR_2 = 0.1034$	$R_1 = 0.0406$ $wR_2 = 0.0906$

Table 2. Selected Bond Distances (Å) and Angles (deg) for Complexes 7, 9, and 10

complex	*d*(Pt−C(1))	*d*(Pt−Cl) *trans* S	*d*(Pt−Cl) *trans* C	tilt angle *θ*[a]	tilt angle *θ*[b]
[(IMes)Pt(dmso)(Cl)$_2$], **7**	1.981(8)	2.310(2)	2.346(2)	67.432	73.400 75.300
[(SIMes)Pt(dmso)(Cl)$_2$], **9**	1.993(4)	2.315(1)	2.342(1)	65.154	76.769 79.216
[(TTP)Pt(dmso)(Cl)$_2$], **10**	1.970(3)	2.3192(8)	2.3458(7)	67.1(3)	45.2(4) 56.6(4)

[a] Tilt angle between platinum coordination plane and NHC imidazole ring. [b]Tilt angle between the imidazole ring and the phenyl substituents.

the angle perturbation is only 1.5° from the expected 90°. The imidazole ring is tilted by some 66° relative to the square-planar coordination sphere of the platinum (Figure 4).

In the IMes-bearing complex **7** and SIMes **9**, the two phenyl rings are staggered and almost perpendicular to the imidazolium ring with a tilt angle in the range 10−18°. The staggered phenyl rings feature is also present in other NHC transition metal complexes.[6d] The dmso molecule is coordinated via the S atom, and in order to minimize the steric congestion about the metal center, the oxygen atom lies in the platinum coordination plane with the two methyl groups placed above and below this plane (Figure 4). The Pt−C(1) distances lie in the range of previously reported NHC(Pt)^{II} complexes,[13] the shortest bond being the one observed for the TTP complex **10**, $d = 1.970(3)$ Å. The absence of substituent on the phenyl ring of the TTP permits the ligand to have a closer contact with the platinum metal center, resulting in a shorter M−C bond length.

In principle, analysis of the Pt−Cl distances should allow for the determination of the position of the NHC ligands on the *trans* influence ligand scale.[11] The higher the position in the *trans* influence scale, the more destabilized the *trans* ligand is. Since the Pt−Cl distance is highly sensitive to the nature of the ligand located in a *trans* position,[14] the present complexes could be particularly useful for this analysis. In the NHC complexes **7**, **9**, and **10** the Pt−Cl(1) and Pt−Cl(2) distances differ by some 0.03 Å, with the Cl *trans* to the NHC displaying the longer bond. The chlorine *trans* to the dmso displays a bond length of 2.31 Å, which is in agreement with bond lengths for Cl *trans* to dmso found in related complexes.[15] The bond lengths of the chlorine *trans* to the NHC are between 2.342 and 2.346 Å for **7**, **9**, and **10**; unfortunately the differences between saturated and unsaturated NHC−Pt complexes are too small (they fall within the range of experimental error) to allow for conclusions on any difference of *trans* effect between them. Still, we can try to compare these data with similar complexes containing phosphines. We find that the ranges of Pt−Cl bond lengths in both ligand families are very similar. For example, in *cis*-[Pt(Cl)$_2$(PMe$_2$Ph)$_2$][16] the Pt−Cl distances are 2.355(1) and 2.359(1) Å; in *cis*-[Pt(Cl)$_2$(dmso)(PMe$_2$Ph)][15] a value of 2.367(3) Å is found. Conversely in the triphenylphosphine complex *cis*-[Pt(Cl)(PPh$_3$)$_2$(SnCl$_3$)][17] the Pt−Cl bond is shorter, 2.333(2) Å. Hence, it seems that NHC ligands have approximately the same *trans* influence as phosphines.

NMR Characterization. The coordination of the NHC ligands to the platinum is confirmed by the appearance in the ^{13}C NMR spectra of the Pt satellites for the carbenic carbon, due to coupling with the metal. The magnitude of the J_{Pt-C} has allowed us to characterize the electronic environment of these

(13) (a) Liu, S.-T.; Hsieh, T.-Y.; Lee, G.-H.; Peng, S. M. *Organometallics* **1998**, *17*, 993−995. (b) Ku, R.-Z.; Huang, J.-C.; Cho, J.-Y.; Kiang, F.-M.; Reddy, K. R.; Chen Y.-C.; Lee, K.-J.; Lee, J.-H.; Lee, G.-H.; Peng, S.-M.; Liu, S.-T. *Organometallics* **1999**, *18*, 2145−2154. (c) Hasan, M.; Kozhevnikov, I. V.; Siddiqui, M. R. H.; Femoni, C.; Steiner, A.; Winterton, N. *Inorg. Chem.* **2001**, *40*, 795−800. (d) Quezada, C. A.; Garrison, J. C.; Tessier, C. A.; Youngs, W. J. *J. Organomet. Chem.* **2003**, *671*, 183−186.

(14) Kapoor, P. N.; Kakkar, R. *J. Mol. Struct.* **2004**, *479*, 149−156.

(15) Kapoor, P.; Lövqvist, K.; Oskarsson, Å. *J. Mol. Struc.* **1998**, *470*, 39−47.

(16) Attia, W. M.; Balducci, G.; Calligaris, M. *Acta Crystallogr. C43* **1987**, 1053−1055.

(17) Cavinato, G.; De Munno, G.; Lami, M.; Marchionna, M.; Tonioli, L.; Viterbo, D. *J. Organomet. Chem.* **1994**, *466*, 277−282.

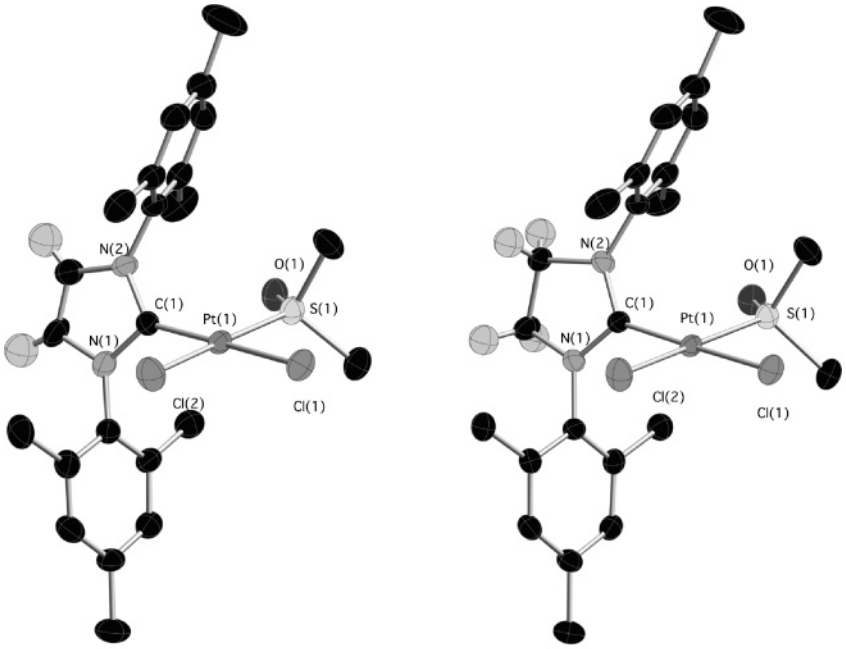

7 9

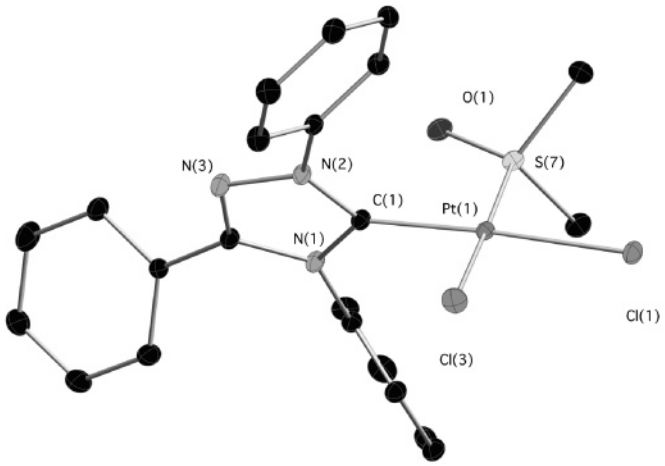

10

Figure 3. Thermal ellipsoid (50% probability) representation of complexes **7**, **9**, and **10**. Hydrogen atoms, except for imidazole ring protons, are omitted for clarity.

compounds (see below). To our knowledge this is the first report of coupling constants between platinum(II) and the carbenic carbon of NHCs.

The coordination of dmso in complexes **6**−**10** is confirmed by the appearance of Pt satellites in both ^{1}H and ^{13}C NMR spectra. The dmso proton signal shifts downfield some 0.2−0.3 ppm with respect to the free dmso ($\delta = 2.62$ ppm), but the shift downfield is about 1 ppm with respect to the starting material [Pt(dmso)$_2$(Cl)$_2$], which appears at 3.56 ppm. The $^{3}J_{\mathrm{Pt-H}}$ values are between 19.3 and 21.4 Hz, slightly smaller than in the starting material ($J = 22.5$ Hz). Complexes **6**−**9** present a downfield shift of the imidazolium ring proton when compared to the chemical shift in the free NHC, indicating a lowering of the electronic charge on the ring associated with the coordination to platinum. As expected, the shift is less than that for the corresponding NHC·HBF$_4$ salts (Table 3).

The ^{1}H NMR spectra of complex **6**−**9** present very insightful features. As revealed by the X-ray structure, the phenyl substituents on the two nitrogens are almost perpendicular to the imidazolium ring and are staggered. The presence of two different ligands *cis* to the carbene (dmso and Cl) makes the *ortho* and *meta* substituents on the phenyl ring inequivalent, as one side of the phenyl ring points to the Cl substituent and the other side to the dmso (see Figure 4). As the rotation of the phenyl is hindered, we observe the duplication of the signals with respect to the free carbene. So for the IMes and SIMes complexes **7** and **9**, the two *meta* protons on the same phenyl ring display two different NMR signals, at 7.07 and 7.03 ppm for **7** and 7.01 and 6.97 ppm for **9**, respectively. Similarly the two methyl groups in the *ortho* position give rise to two different resonances (2.38 and 2.24 ppm for **7** and 2.60 and 2.43 ppm for **9**). The IPr and SIPr complexes **6** and **8** present the same features. Two doublets for the *meta* protons (7.42 and 7.24 ppm for **6**, 7.35 and 7.28 ppm for **8**) and two septuplets for the CH of the isopropyl groups (3.30 and 3.05 ppm for **6**, 3.66 and 3.40 ppm for **8**) are observed. The eight methyl groups of the

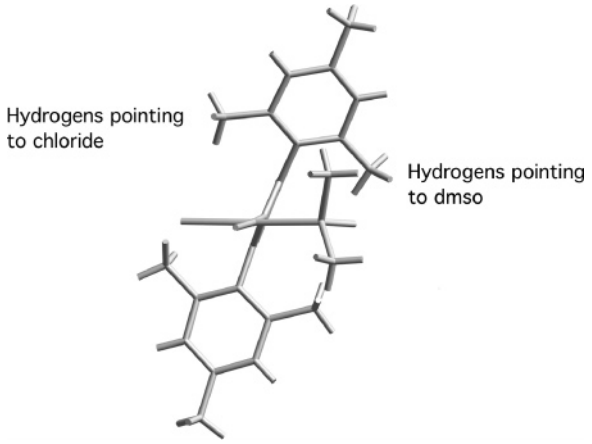

Figure 4. Representation of [(IMes)Pt(dmso)(Cl)$_2$] (**7**) highlighting the tilt angle of the imidazole ring and the diastereotopicity of the hydrogens on the phenyl ring.

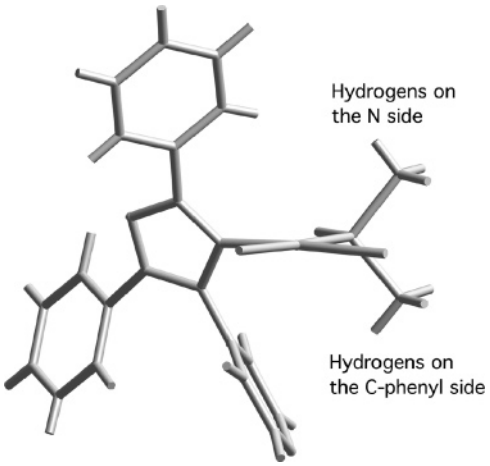

Figure 5. Representation of **10** [(TTP)Pt(dmso)(Cl)$_2$] highlighting the methyl position.

Table 3. ^{1}H NMR Chemical Shifts of NHC Ring Protons

complex	δ_H(complex)[a]	δ_H(NHC)[b]	δ_H(NHC·HBF$_4$)[c]
[(IPr)Pt(dmso)(Cl)$_2$], **6**	7.2	6.73	7.8
[(IMes)Pt(dmso)(Cl)$_2$], **7**	7.1	6.58	8.18
[(SIPr)Pt(dmso)(Cl)$_2$], **8**	4.09	3.47	4.83
[(SIMes)Pt(dmso)(Cl)$_2$], **9**	4.04	3.37	4.74

[a] $CDCl_3$ solution. [b] C_6D_6 solution. [c] $(CD_3)_2CO$ solution.

isopropyl moiety give rise to four doublets, as the two methyl groups of the same isopropyl moiety are nonequivalent. The presence of six resonances for the aromatic phenyl carbon in the ^{13}C NMR spectra for complexes **6**−**9** confirms the asymmetry of the phenyl ring. On the other hand, the ^{13}C NMR spectrum of **10** [(TTP)Pt(dmso)(Cl)$_2$] displays only four resonances for every phenyl ring. Most likely the absence of substituents on the phenyl rings allows free rotation about the C−N and C−C bonds, rendering the *ortho* and *meta* carbons equivalent on the NMR time scale. Complex **10** presents an additional interesting feature: while in all other complexes the two methyl groups of the dmso display just one signal, in the TTP complex **10** two signals, separated by 0.06 ppm, are present (J_{Pt-H} is 20.8 Hz for both signals). Indeed the TTP ligand, due to the presence of a phenyl group on the C3, eliminates the symmetry of the coordination plane of the platinum, rendering the two methyl groups diastereotopic; one is lying on the same side as the phenyl, the other, on the opposite side (Figure 5).

The appearance of two different signals implies that the rotation around the S−Pt bond is hindered at 25 °C on the NMR time scale. In order to determine the rotational barrier of this bond, the complex was dissolved in toluene-d_8 and was then heated in an NMR tube to 110 °C. Even at this temperature, free rotation is not observed. The duplication of the signal of the methyl group of the coordinated dmso is visible also in the ^{13}C NMR spectra, where the two methyl signals have a $\Delta\delta$ of 0.3 ppm. The ^{13}C NMR spectra of complexes **6**−**10** show the peaks of the coordinated dmso at around 45 ppm (shifted 5 ppm with respect to the uncoordinated dmso). The *J* couplings are between 62.0 Hz and 66.9 Hz. The asymmetry of the molecules observed in the ^{1}H NMR spectra is also present in the ^{13}C NMR spectra. For complexes **7** and **9**, the *ortho* and *meta* carbon signals appear as doublets, so that six resonances for the carbons on the aromatic ring and three resonances for the carbon of the methyl moiety are observed. For IPr and SIPr complexes **6** and **8** again six resonances for the aromatic ring and six resonances for the isopropyl moiety are observed. The carbenic carbon chemical shifts of the complexes are shifted upfield when compared to the free carbenes. The values are close to that of the NHC·HCl salts and lie between 145 ppm (unsaturated) and 174 ppm (saturated) (Table 4).

We also observe the ^{195}Pt satellites associated with these resonances. This presents an exceptional opportunity to obtain insights into the electronic distribution among the different components participating in the NHC−Pt bond. Indeed, coupling constants between two nuclei are directly related to the electron density present in the σ orbital of the bond. As the data show, the higher *J* appears for the unsaturated carbene complexes IPr **6** and IMes **7** (1479 Hz and 1472 Hz), then comes the TTP complex **10** (1412 Hz), and finally the saturated carbenes, with a *J* coupling more than 100 Hz lower (1373 Hz for SIPr **8** and 1358 Hz for SIMes **9**). Overall the *J* values decrease in the order IPr > IMes > TTP > SIPr > SIMes. N-Heterocyclic carbenes were usually considered pure σ donors. However, as previously mentioned, recent studies have shown that other types of electronic contribution must be considered when analyzing the NHC−metal bond. Recently, Cavallo and co-workers[18] have reported that about 10% of the electron density of the bond is due to a π-type bond. Among this percentage the contribution of the π back-bond (transfer of the electron density from the metal to the ligand) can reach 80%. To better understand this point, we have also recorded the ^{195}Pt NMR spectra. Indeed, the chemical shift of the platinum center is an indication of the electron density around it: the more downfield the signal, the less electron density on the metal. Our complexes are particularly suitable to study the π back-donation from the metal to the NHC, as all ancillary ligands coordinated do not have this type of contribution in their bonding with the metal. Indeed a similar study on ^{195}Pt chemical shift and J_{Pt-C} has been carried out by Markó et al. on [(NHC)Pt^0(dvtms)] complexes (dvtms = divinyltetramethylsiloxane),[19] but the presence of two alkenes in the coordination sphere of the metal does not allow for any conclusion on the π-accepting ability of the NHC. As a matter of fact the excess electron density on the metal is released onto the coordinated alkenes, notoriously good π acceptors, rendering invisible the π contribution of the NHCs. Moreover no coupling constant between platinum and the carbenic carbon has been reported for IPr, IMes, SIPr, and SIMes, thus not allowing for differentiation between unsaturated and saturated NHCs in this system.

(18) Jacobsen, H.; Correa, A.; Costabile, C.; Cavallo, L. *J. Organomet. Chem.* **2006**, *691*, 4350−4358.

(19) Berthon-Gelloz, G.; Buisine, O.; Brière, J.-F.; Michaud, G.; Stérin, S.; Mignani, G.; Tinant, B.; Declercq J.-P.; Chapon, D.; Markó, I. E. *J. Organomet. Chem.* **2005**, *690*, 6156−6168.

Table 4. ^{13}C and ^{195}Pt NMR Data for (NHC)Pt(II) Complexes[a]

complex	δ_C(NHC)[b]	δ_C(NHC·HBF$_4$)[c]	δ_C(Pt−C(1))[d]	J_{Pt-C}	δ_{Pt}[e]
[(IPr)Pt(dmso)(Cl)$_2$], **6**	220.6	132.2	147.4	1479	1023.3
[(IMes)Pt(dmso)(Cl)$_2$], **7**	219.7	134.8	145.8	1472	1017.0
[(SIPr)Pt(dmso)(Cl)$_2$], **8**	244.0	160.0	174.4	1373	1010.0
[(SIMes)Pt(dmso)(Cl)$_2$], **9**	243.8	160.2	173.8	1358	991.8
[(TTP)Pt(dmso)(Cl)$_2$], **10**	214.2	142.4	153.0	1412	1032.8

[a] δ are in ppm and J_{Pt-C} in Hz. [b] C_6D_6 solution. [c] $(CD_3)_2CO$ solution. [d] $CDCl_3$ solution. [e] CD_2Cl_2 solution.

The ^{195}Pt chemical shifts of complexes **6**−**10** are in the range of 970 ppm and 1050 ppm and in the range of values found for neutral Pt(II) tetracoordinated complexes.[20] The TTP complex **10** has a more deshielded metal center; this can be explained by the substitution in the imidazolium ring of one carbon with the more electronegative nitrogen, with the result that the triazolium ring is less basic than the imidazolium motif.[21] Focusing on the other complexes we find chemical shifts appearing in the following order: IPr **6** (1023.3 ppm) > IMes **7** (1017.0 ppm) > SIPr **8** (1010.0 ppm) > SIMes **9** (991.8 ppm). Indeed there is an average difference of 20 ppm between the chemical shift of unsaturated and saturated carbenes. This is in agreement with the reported feature that replacing a softer ligand with a harder ligand causes a downfield shift of the ^{195}Pt resonance[22] and suggests that the saturated carbenes SIPr and SIMes transfer more electron density onto the metal center than IPr and IMes. Nevertheless the J_{Pt-C} are more than 100 Hz higher for **6** and **7**.

Further information about the different characteristics of the Pt−NHC bond with saturated and unsaturated NHC ligands can be derived from theoretical analysis of the ^{195}Pt NMR data. We calculated the σ isotropic shielding on the Pt atom and the J_{Pt-C} spin−spin coupling constant (see the Computational Details section). Since recent studies evidenced that very accurate results for the ^{195}Pt chemical shifts are possible only in the case of very similar systems, we limited our analysis to a comparison of the SIMes- and IMes-based complexes.[23] The difference between the calculated spin−spin coupling constants and the chemical shielding of compounds **7** and **9** is in good quantitative agreement with the experimental data. This is a consequence of the strict similarity between the two systems investigated.[23] Decomposition of the calculated NMR parameters in terms of the various contributions is reported in Table 5.

In more detail, the calculations correctly reproduce the experimental finding that the Pt center in the IMes-based complex is moved downfield relative to that in the SIMes complex ($\Delta\delta_{Pt} = \sigma^{DFT}$(SIMes) − σ^{DFT}(IMes) = 19 ppm theoretically vs $\Delta\delta_{Pt} = \delta_{Pt}$(IMes) − δ_{Pt}(SIMes) = 25.2 ppm experimentally)[24] and that the Pt−C spin−spin coupling constant in the SIMes-based complex is smaller than in the IMes-based complex ($\Delta J_{Pt-C} = J_{Pt-C}$(SIMes) − J_{Pt-C}(IMes) = 142 Hz theoretically vs 114 Hz experimentally). Decomposition of the calculated shieldings as $\sigma^{DFT} = \sigma^P + \sigma^D + \sigma^{SO}$ indicates that the σ^D contribution is very similar in both systems. The diamagnetic shielding σ^D is essentially a core electron property,

Table 5. Calculated Pt Chemical Shieldings, σ^{DFT}, and Pt−C Spin−Spin Couling Constants, J^{DFT} [a]

Fully Optimized Geometries[b]				
	σ^P (ppm)	σ^D (ppm)	σ^{SO} (ppm)	σ^{DFT} (ppm)
IMes	−7824	9294	3442	4912
SIMes	−7812	9294	3449	4931
	J^P (Hz)	J^D (Hz)	J^{FC} (Hz)	J^{DFT} (Hz)
IMes	−9	0	1609	1600
SIMes	−19	0	1476	1458
Identical Geometry around the Pt Atom[c]				
	σ^P (ppm)	σ^D (ppm)	σ^{SO} (ppm)	σ^{DFT} (ppm)
IMes	−7835	9293	3416	4874
SIMes	−7791	9293	3416	4919
	J^P (Hz)	J^D (Hz)	J^{FC} (Hz)	J^{DFT} (Hz)
IMes	−9	0	1563	1554
SIMes	−19	0	1512	1493

[a] σ^P, σ^D, and σ^{SO} are the paramagnetic, diamagnetic, and spin−orbit contributions to σ^{DFT}. J^P, J^D, and J^{FC} are the paramagnetic, diamagnetic, and Fermi contact contributions to J^{DFT}. [b] Fully optimized geometry data refer to structures obtained with no constraint. [c] Identical geometry around the Pt atom data refers to structures in which the positions of the Pt, Cl, S, and C(carbene) atoms in the two fully optimized geometries have been averaged.

and thus in strictly related systems, as those investigated here, it is reasonable that the difference in σ^D is negligible.[25]

The paramagnetic and the spin−orbit σ^P and σ^{SO} terms both contribute to the higher σ^{DFT} shielding of the SIMes-based system, although the σ^P term is dominating. In a previous study focused on the prediction of the ^{195}Pt chemical shift in [PtX$_2$L$_2$] complexes (X = halogen, L = SMe$_2$, NH$_3$, PMe$_3$),[26] Gilbert and Ziegler evidenced that replacing PMe$_3$ with NH$_3$ causes a largely more negative σ^P term, which results in a more shielded Pt center in the [Pt(Cl)$_2$(PMe$_3$)$_2$] complex. This was attributed to a preference of the soft acid Pt(II) for the softer base PMe$_3$. Similar reasoning can be applied here, considering that SIMes is a softer base than IMes. The spin−orbit σ^{SO} contribution, instead, is usually associated with the involvement of valence s orbitals on the NMR-active atom, Pt in this case, in bonding to other atoms. More s character allows for a better transfer of spin density between the atoms, which results in higher shielding.[27] The small, higher σ^{SO} contribution to the Pt atom in the SIMes-based system might suggest that the Pt−L (L = Cl, dmso, NHC) bonds present a slightly higher s character on the Pt atom. At the same time, it was clearly shown that both the σ^P and σ^{SO} contributions to the shielding of the metal are very sensitive to the M−L bond lengths[28] and that differences

(20) Pregosin, P. S. *Coord. Chem. Rev.* **1982**, *44*, 247−291.
(21) Vianello, R; Maksic, Z. B. *Mol. Phys.* **2005**, *103*, 209−219.
(22) Pregosin P. S. *Annual Reports on NMR Spectroscopy*; Webb, G. A., Ed.; Academic Press: London, 1986; Vol. 17, pp 285−349.
(23) (a) Autschbach J.; Le Guennic B. *Chem.−Eur. J.* **2004**, *10*, 2581−2589. (b) Sterzel, M.; Autschbach, J. *Inorg. Chem.* **2006**, *45*, 3316−3324. (c) Fowe, E. P.; Belser, P.; Daul, C.; Chermette, H. *Phys. Chem. Chem. Phys.* **2005**, *7*, 1732−1738.
(24) Assuming that the Pt chemical shift δ_{Pt} is given by the difference between the chemical shieldings σ_{Pt} of the reference and of the probe, δ_{Pt}(NHC) = σ_{Pt}(PtCl$_6^{2-}$) − σ_{Pt}(NHC), we have: $\Delta\delta_{Pt}$(IMes − SIMes) = δ_{Pt}(IMes) − δ_{Pt}(SIMes) = σ_{Pt}(PtCl$_6^{2-}$) − σ_{Pt}(IMes) − (σ_{Pt}(PtCl$_6^{2-}$) − σ_{Pt}(SIMes)) = σ_{Pt}(SIMes) − σ_{Pt}(IMes).
(25) Austchbach, J.; Ziegler, T. *Encyclopedia of Nuclear Magnetic Resonance, Advances in NMR*; John Wiley and Sons Ed.: Chichester, UK, 2002; Vol. 9, p 306.
(26) Gilbert, T. M.; Ziegler, T. *J. Phys. Chem. A* **1999**, *103*, 7535−7543.
(27) Kaupp, M.; Malkina, O. L.; Malkin, V. G.; Pyykkö. *Chem.−Eur. J.* **1998**, *4*,118−126.
(28) Wolff, S. K.; Ziegler, T.; van Lenthe, E.; Baerends, E. J. *J. Chem. Phys.* **1999**, *110*, 7689−7698.

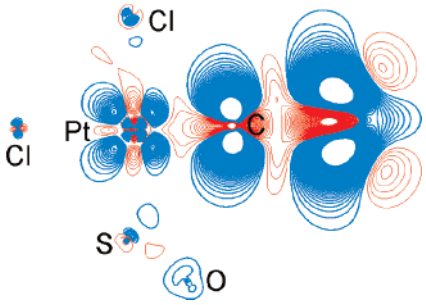

Figure 6. Electron density difference, $\Delta\rho^{S-I} = \rho^{SIMes} - \rho^{IMes}$, between the SIMes and IMes (NHC)$PtCl_2$(dmso) systems. Red curves and blue curves refer to $\Delta\rho^{S-I} > 0$ and < 0, respectively. Isodensity curves are drawn every 0.002 au.

in the bond lengths of 0.01 Å can result in shielding differences of 20−30 ppm. For this reason, we performed further calculations on complexes having exactly the same geometry of coordination at the Pt atom, by averaging the position of the Cl, S, and C(carbene) atoms in the SIMes and IMes fully optimized systems. This way, any difference in the DFT chemical shielding of Pt in the IMes- and SIMes-based complexes is a consequence of the different nature of the NHC ligand. These calculations, reported in Table 5, confirm that the σ^P term is less negative in the SIMes-based system, which corresponds to a more shielded Pt atom in this complex. This confirms that the SIMes ligand can be considered a softer donor compared to the IMes ligand. At the same time, the calculations also indicate that the σ^{SO} term is essentially identical in the two systems when the geometry around the Pt atom is identical, which suggests that the small difference in the σ^{SO} observed in the case of fully optimized geometries is due to small geometrical differences.

Focusing on the Pt−NHC spin−spin coupling constant, usually considered a valence property, decomposition of the calculated J_{Pt-C} couplings as $J^{DFT} = J^P + J^D + J^{FC}$ indicates that the difference in the coupling between the Pt and the SIMes and IMes ligands is completely dominated by the Fermi contact term J^{FC}. As for the chemical shielding, this term is associated with a transfer of spin density through the bond, and it has been shown that only molecular orbitals with σ-type components contribute to the coupling.[27] This suggests that the Pt−IMes bond has a higher σ character than the Pt−SIMes bond. Also in this case we performed test calculations of the coupling constants, in which we imposed identical geometry of coordination at the Pt atom. The resulting J_{Pt-C}, reported in Table 4, indicate that a higher J_{Pt-C} is predicted for the IMes-based system even in the case of identical geometry around the Pt center, which supports our proposal that the Pt−IMes bond has a higher σ character than the Pt−SIMes bond.

Analysis of the electron density ρ in the SIMes- and IMes-based systems supports this rationalization of the NMR data. Figure 6 reports the electron density difference $\Delta\rho^{S-I}$ between SIMes and IMes systems in the IMes and SIMes complexes. To avoid ambiguities, we used again identical coordination geometry around the Pt center, by averaging the position of the Pt, Cl, S, and C(carbene) atoms in the fully optimized complexes. Red lines indicate areas where $\rho^{SIMes} > \rho^{IMes}$, while blue lines indicate areas where $\rho^{IMes} > \rho^{SIMes}$. Looking at Figure 6 it is clear that the distribution of electron density is rather different between the SIMes- and the IMes-based systems. Specifically, it is clear that the C(carbene) atom of the SIMes ligand is a better σ donor than the IMes ligand, since there is more electron density along the Pt−SIMes bond (see the red curves emerging from the C(carbene) and oriented along the SIMes−Pt bond). Very interestingly, the plot also indicates that there is higher density along the Pt−Cl and Pt−S bonds (see the red curves emerging from Pt and oriented along the Pt−C and Pt−S bonds). This indicates that the higher σ donicity of the SIMes ligand pushes σ electron density of the metal atom away from the Pt−SIMes bond, toward the other ligands to the Pt center. This accumulation (depletion) of electron density close to the C (Pt) atom suggests that the Pt−SIMes bond is more polarized than the Pt−IMes bond. The plot of Figure 6 also indicates a reduction of electron density at the Pt atom of the SIMes system, corresponding to d orbitals (blue curves). This is indicative of stronger d→π* back-bonding in the SIMes system, because there is depletion of π density at the Pt atom. Blue curves around the C(carbene) atom, which indicate that less π electron density is localized also on the C(carbene) of the SIMes ring, are not easily rationalized, since the C(carbene) atom in the SIMes and IMes rings participates in different π orbital schemes.

In short, analysis of the electron density supports the NMR analysis. In fact, the SIMes ligand is shown to be a softer and more donating base than the IMes ligand, which explains the more shielded Pt atom in the SIMes-based system, while polarization of the σ density on the Pt atom, away from the SIMes ligand and toward the Pt−Cl and Pt−S bonds, explains the reduced Pt−C spin−spin coupling constant in the SIMes-based system. We further note that some of us previously suggested that the experimentally observed better binding properties of unsaturated [(NHC)$Ru(Cl)_2$]-based systems relative to the saturated analogues[29] were due to the higher *trans* effect of saturated NHC ligands.[30] The experimental and theoretical analysis we performed here provide a mechanistic basis for a phenomenon that is probably general. The higher σ donicity of the SIMes ligand causes the metal center to be a weaker σ acceptor (toward ligands other than the NHC), while the increased Pt−NHC d→π* back-bonding in the case of the SIMes ligand causes the metal to be a weaker π donor (toward ligands other than the NHC). Experimental support for this analysis also stems from a study of [(NHC)$Ni(CO)_3$] complexes, where the interaction of the σ donor and π acceptor CO ligand with the metal center was investigated. The experimental IR CO stretching frequencies in the IMes-based system were measured to be 1−2 cm^{-1} smaller than in the SIMes-based system, while the DFT binding energy of CO in the IMes-based system was calculated to be 1.5 kcal/mol higher than in the SIMes-based system.[6d] This might explain the different catalytic performances of systems based on saturated and unsaturated NHC ligands.

Finally, we performed an energy decomposition analysis commonly used to estimate the amount of σ donation and d→π* back-bonding in M−NHC bonds.[31] This analysis is usually done by taking advantage of symmetry constraints on the complex.[8c,18] If the NHC ring lies in a symmetry plane, within C_s symmetry the σ and π Pt−NHC bonds belong to the a′ and a″ irreducible representations, respectively, see Scheme 1. In the *cis*-(NHC)-Pt(dmso)Cl_2 complex, which can be considered to be C_s symmetric, the *yz* symmetry plane is orthogonal to the NHC ring and corresponds to the coordination plane of the Pt center. Unfortunately, in this case both the σ and π Pt−NHC bonds belong to the a′ irreducible representation, and thus no sym-

(29) Sanford, M. S.; Love, J. A.; Grubbs, R. H. *J. Am. Chem. Soc.* **2001**, *123*, 6543−6554.
(30) Cavallo, L. *J. Am. Chem. Soc.* **2002**, *124*, 8965−8973.
(31) (a) Ziegler, T. NATO ASI C 378, 1992; p 367. (b) Jacobsen, H.; Ziegler, T. *Comments Inorg. Chem.* **1995**, *17*, 301−317. (c) Ziegler, T.; Rauk, A. *Inorg. Chem.* **1979**, *18*, 1558−1565.

Scheme 1

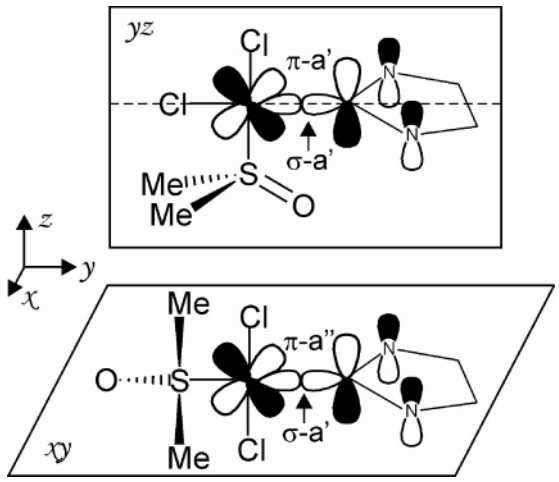

metry-based argument can be applied. However, the *trans*-[(NHC)Pt(dmso)$(Cl)_2$] complex, which can also be considered to be C_s symmetric, presents the *xy* symmetry plane coincident to the NHC ring and orthogonal to the coordination plane of the Pt center. This allows to separate the σ and π Pt−NHC bonds by symmetry. We thus optimized both the *cis* and *trans* geometries of the IMes- and SIMes-based complexes imposing C_s symmetry. For both the NHC ligands the *trans* complex is about 15 kJ/mol higher in energy than the *cis* complex. This suggests that the bonding scheme in the *cis* and *trans* geometries is rather similar, and analysis of the *trans* geometries offers information that can be reasonably transferred to the experimental *cis* geometries. This analysis indicates that in both the SIMes- and IMes-based complexes the d→π* back-donation amounts to roughly 13% of the total orbital interaction energy. The SIMes system presents a σ contribution 5 kJ/mol higher than the IMes system, consistent with the higher donicity expected for the SIMes ligand. Also the d→π* back-donation is higher in the SIMes system, although by only 1 kJ/mol. Overall, the Pt−NHC bond is roughly 6 kJ/mol stronger with the SIMes ligand than with the IMes ligand.

Conclusions

In order to gain insight into the stereoelectronic properties of the NHC ligands, we have reported the synthesis and detailed structural and NMR studies of [(NHC)Pt^{II}] compounds. From the analysis of the X-ray structures, we observed that the NHC ligands used in the present study have almost the same *trans* influence as tertiary phosphines. Unfortunately, the differences in the Pt−Cl bond distances are too small to allow for a differentiation between saturated and unsaturated NHC.

Combining the ^{195}Pt chemical shift data, the J_{Pt-C} values, and the theoretical calculations, we are able to provide an improved description of the bond between NHCs and the metal. Notably, we are able to state that NHCs are not to be considered as pure σ donors. Indeed, π back-donation contributes 13% to the character of the bond. Keeping in mind that in our study the platinum is in a +2 oxidation state, the percentage of π back-donation could significantly increase for more electron-rich metals. Of course in the present system no strongly π-accepting ligands are present. Saturated NHCs bind to the metal stronger than the corresponding unsaturated NHC, in accordance with previously reported results. Electron density analysis indicates that more electron density is back-donated from the Pt center to saturated NHCs than to unsaturated NHCs. Unsaturated NHCs, IPr and IMes, are thus both less σ donating and less efficient π acceptors. The result is that they are weaker ligands and leave the metal center more electron poor than their saturated congeners.

This analysis finally helps explain why in some catalytic systems ligands varying from saturated to unsaturated NHCs heavily affect the catalytic activity. The unsaturated carbenes make the metal center a better σ acceptor and π donor, which renders coordination of substrates usually more facile (the exact behavior also depends on substrate electronics as well). However, due to the weaker bond they form with the metal, this could give rise to stability issues. Conversely, saturated NHCs, more strongly bound ligands, stabilize the catalyst but may also lower its reactivity, probably because they make the metal center a worse σ acceptor and π donor, which results in weaker interaction with many substrates. The present study provides a clearer picture of the bonding involved in the metal−NHC interaction. The specific experiments allow for a better understanding of the coordination mode of this class of ligand.

Experimental Section

All reactions were carried out in a MBraun glovebox containing dry argon and less than 1 ppm of oxygen. Anhydrous solvents were either distilled from appropriate drying agents or purchased from Aldrich and degassed prior to use by purging with dry argon and kept over molecular sieves. Solvents for NMR spectroscopy were degassed with argon and dried over molecular sieves. NMR spectra were collected on 300 and 400 MHz Bruker spectrometers. Elemental analyses were performed by Robertson Microlit Labs. Exact mass measurements were performed on a ESI-TOF Waters LCT Premier instrument. The *cis*-[Pt(dmso)$_2$(Cl)$_2$][32] and NHC ligands **1**−**4**,[33] **5**,[34] and **6**[35] were synthesized according to literature procedures. ^{195}Pt spectra were calibrated with $Na_2[PtCl_6]$ in D_2O at 4522 ppm.

Synthesis of [Pt(IPr)(dmso)$(Cl)_2$] (6). In a 50 mL Schlenk flask, 318 mg (0.75 mmol) of [Pt(dmso)$_2$(Cl)$_2$] is suspended in 25 mL of THF; a solution of 351 mg (0.90 mmol) of IPr in 6 mL of THF is added to the slurry, which is then stirred for 3 h at room temperature. During this time, the [Pt(dmso)$_2$(Cl)$_2$] gradually dissolved, giving rise to a yellow pale solution. Afterward the THF is evaporated and to the residue is added 5 mL of acetone. A white solid is collected by filtration. Addition of pentane (15 mL) to the acetone solution affords more product (total yield of two crops: 460 mg, 84% yield). ^{1}H NMR ($CDCl_3$, 300 MHz): δ 7.53 (t, J = 7.7 Hz, 2H, C*H* aromatic), 7.42 (dd, J = 7.7 Hz, J = 1.3 Hz, 2H, C*H* aromatic), 7.24 (dd, J = 7.7 Hz, J = 1.3 Hz, 2H, C*H* aromatic), 7.20 (s, 2H, C*H* imidazole), 3.30 (septet, J = 6.7 Hz, 2H, C*H*$(CH_3)_2$), 3.05 (septet, J = 6.7 Hz, 2H, C*H*$(CH_3)_2$), 2.84 (s, J_{Pt-H}= 19.3 Hz, 6H, C*H*$_3$ dmso), 1.51 (d, J = 6.7 Hz, 6H, CH(C*H*$_3$)$_2$), 1.39 (d, J = 6.7 Hz, 6H, CH(C*H*$_3$)$_2$), 1.12 (d, J = 6.7 Hz, 6H, CH(C*H*$_3$)$_2$), 1.08 (d, J = 6.7 Hz, 6H, CH(C*H*$_3$)$_2$). ^{13}C NMR ($CDCl_3$, 300 MHz): δ 148.50 (s, *C* aromatic), 147.38 (s, J_{Pt-C}= 1479 Hz, *C* carbene), 146.45 (s, *C* aromatic), 135.15 (s, *C* aromatic), 130.88 (s, *C*H aromatic), 125.26 (s, *C*H aromatic), 124.55 (s, J_{Pt-C}= 39.6 Hz, *C*H imidazole), 124.19 (s, *C*H aromatic), 45.46 (s, J_{Pt-C} = 64 Hz, *C*H$_3$ dmso), 29.46 (s, *C*H$(CH_3)_2$), 28.79 (s, *C*H$(CH_3)_2$), 27.00 (s, CH(*C*H$_3$)$_2$), 26.93 (s, CH(*C*H$_3$)$_2$), 23.58 (s, CH(*C*H$_3$)$_2$),

(32) Romeo, R.; Scolaro, L. M. *Inorg. Synt.* **1998**, *32*, 153−158.
(33) Arduengo, A. J., III; Krafczyk, R.; Schmutzler, R.; Craig, H. A.; Goerlich, J. R.; Marshall, W. J.; Unverzagt, M. *Tetrahedron* **1999**, *55*, 14523−14534.
(34) Kuhn, N.; Kratz, T. *Synthesis* **1993**, 561−562.
(35) Enders, D.; Breuer, K.; Kallfass, U.; Balensiefer, T. *Synthesis* **2003**, 1292−1295.

23.10 (s, CH(CH_3)$_2$). ^{195}Pt NMR (CD_2Cl_2, 400 MHz): 1023.34 ppm. Anal. Calcd for $C_{29}H_{43}Cl_2N_2OPtS$ (MW: 733.71): C, 47.47; H, 5.91; N, 3.82. Found: C, 47.49; H, 5.65; N, 3.73.

Synthesis of [Pt(IMes)(dmso)(Cl)$_2$] (7). In a 50 mL Schlenk flask 220 mg (0.52 mmol) of [Pt(dmso)$_2$(Cl)$_2$] is suspended in 20 mL of THF; a solution of 174 mg (0.57 mmol) of IMes in 5 mL of THF is added to the slurry, which is then stirred for 2 h at room temperature. During this time, the [Pt(dmso)$_2$(Cl)$_2$] gradually dissolved, giving rise to a yellow pale solution. The THF is removed in vacuo, and to the residue 4 mL of acetone is added. A white solid is collected by filtration. Addition of pentane (15 mL) to the acetone solution affords more product (total combined yield of both crops: 337 mg, 86% yield). ^{1}H NMR ($CDCl_3$, 300 MHz): δ 7.10 (s, 2H, C*H* imidazole), 7.07 (s, 2H, C*H* aromatic), 7.03 (s, 2H, C*H* aromatic), 2.95 (s, J_{Pt-H} = 20.7 Hz, 6H, CH_3 dmso), 2.42 (s, 6H, CH_3), 2.38 (s, 6H, CH_3), 2.24 (s, 6H, CH_3). ^{13}C NMR ($CDCl_3$, 300 MHz): δ 145.82 (s, J_{Pt-C}= 1471.9 Hz, *C* carbene), 139.78 (s, *C* aromatic), 137.25 (s, *C* aromatic), 135.77 (s, *C* aromatic), 134.97 (s, *C* aromatic), 130.26 (s, *C*H aromatic), 129.49 (s, *C*H aromatic), 123.78 (s, J_{Pt-C} = 39.8 Hz, *C*H imidazole), 45.57 (s, J_{Pt-C} = 64.8 Hz, *C*H$_3$ dmso), 21.50 (s, *C*H$_3$), 20.44 (s, *C*H$_3$), 19.36 (s, *C*H$_3$). ^{195}Pt NMR (CD_2Cl_2, 400 MHz): 1016.97 ppm. Anal. Calcd for $C_{23}H_{31}Cl_2N_2OPtS$ (MW: 649.55): C, 42.53; H, 4.81; N, 4.31. Found: C, 42.96; H, 4.38; N, 4.21.

Synthesis of [Pt(SIPr)(dmso)(Cl)$_2$] (8). In a 50 mL Schlenk flask, 305 mg (0.72 mmol) of [Pt(dmso)$_2$(Cl)$_2$] is suspended in 25 mL of THF; a solution of 284 mg (0.73 mmol) of SIPr in 6 mL of THF is added to the slurry, which is then stirred for 3 h at room temperature. During this time, the [Pt(dmso)$_2$(Cl)$_2$] gradually dissolved, giving rise to a yellow pale solution. The THF is then evaporated and the residue triturated with 5 mL of ethanol. A white product is then collected by filtration (280 mg, 53% yield). ^{1}H NMR ($CDCl_3$, 300 MHz): δ 7.44 (t, J = 7.6 Hz, 2H, C*H* aromatic), 7.35 (dd, J = 7.6 Hz, J = 1.4 Hz, 2H, C*H* aromatic), 7.28 (dd, J = 7.6 Hz, J = 1.4 Hz, 2H, C*H* aromatic), 4.10 (m, 4H, CH_2 imidazole), 3.66 (septet, J = 6.7 Hz, 2H, C*H*(CH$_3$)$_2$), 3.40 (septet, J = 6.7 Hz, 2H, C*H*(CH$_3$)$_2$), 2.78 (s, J_{Pt-H}= 19.6 Hz, 6H, CH_3 dmso), 1.56 (d, J = 6.7 Hz, 6H, CH(CH_3)$_2$), 1.47 (d, J = 6.7 Hz, 6H, CH(CH_3)$_2$), 1.23 (d, J = 6.7 Hz, 12H, CH(CH_3)$_2$). ^{13}C NMR ($CDCl_3$, 300 MHz): δ 174.41 (s, J_{Pt-C} = 1373 Hz, *C* carbene), 149.00 (s, *C* aromatic), 147.39 (s, *C* aromatic), 135.44 (s, *C* aromatic), 130.08 (s, *C*H aromatic), 125.62 (s, *C*H aromatic), 124.61 (s, *C*H aromatic), 54.23 (s, J_{Pt-C} = 50 Hz, *C*H$_2$ imidazole), 45.60 (s, J_{Pt-H} = 62 Hz, *C*H$_3$ dmso), 29.57 (s, *C*H(CH$_3$)$_2$), 28.85 (s, *C*H(CH$_3$)$_2$), 27.63 (s, CH(*C*H$_3$)$_2$), 27.54 (s, CH(*C*H$_3$)$_2$), 24.37 (s, CH(*C*H$_3$)$_2$), 24.23(s, CH-(*C*H$_3$)$_2$). ^{195}Pt NMR (CD_2Cl_2, 400 MHz): 1009.96 ppm. Anal. Calcd for $C_{29}H_{45}Cl_2N_2OPtS$ (MW: 735.73): C, 47.34; H, 6.16; N, 3.81. Found: C, 47.27; H, 6.03; N, 3.70.

Synthesis of [Pt(SIMes)(dmso)(Cl)$_2$] (9). In a 50 mL Schlenk flask, 309 mg (0.73 mmol) of [Pt(dmso)$_2$(Cl)$_2$] is suspended in 20 mL of THF; a solution of 228 mg (0.74 mmol) of SIMes in 5 mL of THF is added to the slurry, which is then stirred for 3 h at room temperature. During this time, the [Pt(dmso)$_2$(Cl)$_2$] gradually dissolved and a white precipitate formed. The solid is filtrated and washed with hexane (350 mg, 74% yield). ^{1}H NMR ($CDCl_3$, 300 MHz): δ 7.01 (s, 2H, C*H* aromatic), 6.97 (s, 2H, C*H* aromatic), 4.03 (m, 4H, CH_2 imidazole), 2.92 (s, J_{Pt-H}= 21.4 Hz, 6H, CH_3 dmso), 2.60 (s, 6H, CH_3), 2.43 (s, 6H, CH_3), 2.33 (s, 6H, CH_3). ^{13}C NMR ($CDCl_3$, 300 MHz): δ 172.83 (s, J_{Pt-C} = 1358.0, *C* carbene), 139.10 (s, *C* aromatic), 137.93 (s, *C* aromatic), 136.73 (s, *C* aromatic), 135.11 (s, *C* aromatic), 130.15 (s, *C*H aromatic), 129.70 (s, *C*H aromatic), 51.86 (s, J_{Pt-C} = 44.5 Hz, *C*H$_2$ imidazole), 45.50 (s+sat, J_{Pt-C} = 66.2 Hz, *C*H$_3$ dmso), 21.18 (s, *C*H$_3$), 20.20 (s, *C*H$_3$), 19.06 (s, *C*H$_3$). ^{195}Pt NMR (CD_2Cl_2, 400 MHz): 991.76 ppm. Anal. Calcd for $C_{23}H_{33}Cl_2N_2OPtS$ (MW: 651.57): C, 42.40; H, 5.10; N, 4.30. Found: C, 42.20; H, 4.84; N, 4.19.

Synthesis of [Pt(TTP)(dmso)(Cl)$_2$] (10). In a 50 mL Schlenk flask, 104 mg (0.246 mmol) of [Pt(dmso)$_2$(Cl)$_2$] is suspended in 20 mL of THF; a solution of 74 mg (0.246 mmol) of TTP in 5 mL of THF is added to the slurry, which is then stirred for 3 h at room temperature. During this time, the [Pt(dmso)$_2$(Cl)$_2$] gradually dissolved, giving rise to a yellow solution. Afterward the THF is evaporated and the residue is dissolved in 4 mL of CH_2Cl_2. After the addition of 10 mL of hexane a white product precipitates overnight. The solid is then collected by filtration (140 mg, 89% yield). ^{1}H NMR ($CDCl_3$, 300 MHz): δ 8.27 (d, 2H, CH aromatic), 7.65 (m, 8H, CH aromatic), 7.44 (m, 3H, CH aromatic), 7.33 (m, 2H, CH aromatic), 2.96 (s, J_{Pt-H} = 20.8 Hz, 3H, CH_3 dmso), 2.89 (s, J_{Pt-H} = 20.4 Hz, 3H, CH_3 dmso). ^{13}C NMR ($CDCl_3$, 300 MHz): δ 154.10 (s, J_{Pt-C} = 44.8 Hz, *C* imidazole), 152.99 (s, J_{Pt-C} = 1412 Hz, *C* carbene), 139.07 (s, *C* aromatic), 136.25 (s, *C* aromatic), 131.74 (s, *C*H aromatic), 130.93 (s, *C*H aromatic), 130.29 (s, *C*H aromatic), 130.23 (s, *C*H aromatic), 129.80 (s, *C*H aromatic), 129.24 (s, *C*H aromatic), 129.17 (s, *C*H aromatic), 128.98 (s, *C*H aromatic), 126.12 (s, *C*H aromatic), 124.38 (s, *C* aromatic), 45.55 (s, J_{Pt-C} = 66.9 Hz, *C*H$_3$ dmso), 45.25 (s, J_{Pt-C} = 66.4 Hz, *C*H$_3$ dmso). ^{195}Pt NMR (CD_2Cl_2, 400 MHz): 1032.82 ppm. Anal. Calcd for $C_{22}H_{22}Cl_2N_3OPtS$ (MW: 642.48): C, 41.13; H, 3.45; N, 6.54. Found: C, 40.85; H, 3.18; N, 6.32.

Synthesis of TTP·HBF$_4$. In a Schlenk flask TTPOMe (124.6 mg, 0.379 mmol) is heated under vaccum at 80 °C overnight. After dissolution in 5 mL of THF, a suspension of NH_4BF_4 (79.5 mg, 0.759 mmol) in 15 mL of THF is added. The slurry is stirred at room temperature for 24 h. During this time, a white solid precipitates. Filtration affords 110 mg of the product (76% yield). ^{1}H NMR ((CD$_3$)$_2$CO, 400 MHz): δ 10.93 (s, 1H, C*H* imidaz), 8.18 (d, J = 7 Hz, 2H, C*H* arom), 7.75 (m, 11H, C*H* arom), 7.56 (t, J = 7 Hz, 2H, C*H* arom). ^{13}C NMR ((CD$_3$)$_2$CO, 400 MHz): δ 154.36 (s, *C* arom), 142.39 (s, *C*H imidaz), 135.34 (s, *C* arom), 132.38 (s, *C* arom), 132.36 (s, *C*H arom), 131.62 (s, *C*H arom), 131.08 (s, *C*H arom), 130.31 (s, *C*H arom), 130.28 (s, *C*H arom), 129.63 (s, *C*H arom), 129.15 (s, *C*H arom), 126.64 (s, *C*H arom), 122.74 (s, *C* imidaz), 121.28 (s, *C*H arom). ^{11}B NMR ((CD$_3$)$_2$CO, 400 MHz): δ −1.04 (quint, J = 0.5 Hz). ^{19}F NMR ((CD$_3$)$_2$CO, 400 MHz): δ −151.4 (s). Exact mass determination for $C_{20}H_{16}N_3$ (298.1344): 298.1331.

Computational Details. All calculations were performed with the ADF 2006 package.[36] The generalized gradient-corrected BP86 functional was used.[37] *Trans* and *cis* geometries of the Pt(NHC)-(dmso)Cl$_2$ complexes, used to evaluate the σ and π contributions to the total orbital interaction energy, were optimized in the gas phase, and C_s symmetry was imposed to the complexes. Scalar relativistic effects were included with the ZORA Hamiltonian.[38] A triple-ζ basis set plus two polarization functions (ZORA/TZ2P basis set in ADF) was adopted for Pt, while for main group atoms we adopted a triple-ζ basis set plus one polarization function (ZORA/TZP basis set in ADF). The frozen core approximation was used for core electrons up to and including 4f for Pt, 2p for S and Cl, and 1s for C and N.

To obtain geometries to be used for the calculation of the shielding and spin−spin coupling constants, we also included solvent effects (dmso) using the continuum solvation model

(36) (a) Fonseca Guerra, C.; Snijders, J. G.; te Velde, G.; Baerends, E. J. *Theor. Chem. Acc.* **1998**, *99*, 391−403. (b) te Velde, G.; Bickelhaupt, F. M.; Baerends, E. J.; Fonseca Guerra, C.; van Gisbergen, S. J. A.; Snijders, J. G.; Ziegler, T. *J. Comput. Chem.* **2001**, *22*, 931−967. (c) ADF2005.01, SCM, Theoretical Chemistry, Vrije Universiteit, Amsterdam, The Netherlands, http://www.scm.com.)

(37) (a) Becke, A. D. *Phys. Rev. A* **1988**, *38*, 3098−3100. (b) Perdew, J. P. *Phys. Rev. B* **1986**, *33*, 8822−8824, and corrigendum: Perdew, J. P. *Phys. Rev. B* **1986**, *34*, 7406.

(38) (a) van Lenthe, E.; Baerends, E. J.; Snijders, J. G. *J. Chem. Phys.* **1993**, *99*, 4597−4610. (b) van Lenthe, E.; Baerends, E. J.; Snijders, J. G. *J. Chem. Phys.* **1994**, *101*, 9783−9792. (c) van Lenthe, E.; Ehlers, A. E. Baerends, E. J. *J. Chem. Phys.* **1999**, *110*, 8943−8953.

COSMO,[39] with a dielectric constant $\epsilon = 3.17$ and with a solvent radius of 4.8 Å. To build the cavity, the following atomic radii, 1.16, 2.20, 1.40, 1.30, 2.30, 2.30, and 1.76 Å, were used for H, C, N, S, Cl, and Pt. No symmetry constraints were applied. The Pt shielding and the J_{Pt-C} spin−spin coupling constants were calculated on the optimized geometries using ZORA/TZ2P all-electron basis sets for main group atoms. For Pt we used a specifically tuned all-electrons basis set.[23b] For the calculations of the Pt shielding, and for the electron density analysis, we first performed a single-point ADF calculation on the optimized geometries using the all-electron basis sets, with inclusion of spin−orbit relativistic effects (ZORA) and with dmso (COSMO) as solvent. Default input to the NMR program[40] in the ADF package was used. For the calculations of the J_{Pt-C} spin−spin coupling constant we performed a single-point ADF calculation on the optimized geometries, using the all-electrons basis set, with inclusion of scalar relativistic effects based on the ZORA Hamiltonian and with dmso (COSMO) as solvent. The input to the CPL program[41] in the ADF package consisted in the calculation of the paramagnetic and diamagnetic orbital terms (PMO and DMO keywords) and of the Fermi contact term (FC keyword).

Acknowledgment. The ICIQ Foundation, The Petroleum Research Fund administered by the ACS, the Ministerio de Educación y Ciencia (Spain), and ICREA (SPN is ICREA Research Professor) are gratefully acknowledged for support. The MIUR is gratefully thanked for a Ph.D. grant to S.F. We thank Umicore AG and Lilly for generous gifts of reagents. Degussa A. G. is gratefully acknowledged for gift of 1,3,4-triphenyl-4,5-dihydro-1*H*-1,2,4-triazol-2-ylidene precursor. L.C. thanks CINECA (INSTM grant) for computer time.

Supporting Information Available: Crystallographic information files (CIF) for complexes **7**, **9**, and **10**. This material is available free of charge via the Internet at http://pubs.acs.org. Crystallographic data have been deposited at the CCDC, 12 Union Road, Cambridge CB2 1EZ, U.K., and can be obtained on request, free of charge, by quoting the publication citation and the deposition numbers 630115 (**10**), 630116 (**7**), and 630117 (**9**).

OM700857J

(39) Klamt, A.; Schüürmann, J. *J. Chem. Soc., Perkin Trans. 2* **1993**, 799−805. (b) Pye, C. C.; Ziegler, T. *Theor. Chem. Acc.* **1999**, *101*, 396−408.

(40) Schreckenbach, G.; Ziegler, T. *J. Phys. Chem.* **1995**, *99*, 606−611.

(41) (a) Autschbach, J.; Ziegler, T. *J. Chem. Phys.* **2000**, *113*, 936−947. (b) Autschbach, J.; Ziegler, T. *J. Chem. Phys.* **2000**, *113*, 9410−9418.